Are Cerium Oxide Nanoparticles Transferred from Plants to the Aphid Myzus persicae (Hemiptera: Aphididae)?

Authors: Marucci, Rosangela Cristina, Freitas, Larah Martins, Santos-Rasera, Joyce Ribeiro, Alves, Dejane Santos, Carvalho, Geraldo Andrade, et al.

Source: Florida Entomologist, 102(3) : 555-561

Published By: Florida Entomological Society

URL: https://doi.org/10.1653/024.102.0338

Are cerium oxide nanoparticles transferred from plants to the aphid *Myzus persicae* (Hemiptera: Aphididae)?

Rosangela Cristina Marucci[1,], Larah Martins Freitas[1], Joyce Ribeiro Santos-Rasera[2], Dejane Santos Alves[3], Geraldo Andrade Carvalho[1], and Hudson Wallace Pereira de Carvalho[2,*]*

Abstract

In the last 20 yr, the production of nanoparticles has increased, although their effects on organisms and the environment are not well understood. This research evaluated the transfer of cerium oxide (nano-CeO_2) nanoparticles in a terrestrial trophic chain formed by the producer *Nicandra physaloides* (L.) Gaertn. (Solanaceae) and a primary consumer, green peach aphid, *Myzus persicae* (Sulzer) (Hemiptera: Aphididae), a generalist insect pest. *Nicandra physaloides* plants were treated by foliar spraying with nano-CeO_2 (25 nm) aqueous suspensions (1, 10, 100, and 1,000 mg Ce L^{-1}) and fed to the green peach aphid (*M. persicae*). The survival and fecundity of insects were evaluated. Microprobe X-ray fluorescence spectroscopy was used to verify the presence of Ce in plants and insects. It was possible to verify Ce in the oral cavity and digestive system of aphids fed on leaves previously treated with nano-CeO_2 (1,000 mg CeL^{-1}). Despite the transfer of Ce in this terrestrial trophic chain, the nanoparticles did not reduce survival and fecundity of aphids.

Key Words: nanotechnology; Solanaceae; insect; trophic transfer; X-ray fluorescence spectroscopy

Resumo

Nas últimas décadas, a produção de nanopartículas tem aumentado; entretanto, seus efeitos em organismos e no meio ambiente ainda não são bem compreendidos. A transferência de nanopartículas de óxido de cério (Nano-CeO_2) em uma cadeia trófica terrestre, formada pelo produtor *Nicandra physaloides* (L.) Gaertn. (Solanaceae) e pelo consumidor primário, inseto-praga generalista, *Myzus persicae* (Sulz.) (Hemiptera, Aphididae), foi avaliada nesse trabalho. Plantas de *N. physaloides* foram submetidas a tratamento via pulverização foliar com suspensão aquosa de nano-CeO_2, 25 nm (1, 10, 100, e 1.000 mg Ce L^{-1}) e empregadas para alimentação do pulgão verde (*M. persicae*). Empregando-se microanálise por espectroscopia de fluorescência de raios-X foi possível constatar a presença de Ce nas plantas e insetos. Assim, o Ce foi observado na cavidade oral e sistema digestivo dos pulgões que se alimentaram das folhas previamente tratadas com nano-CeO_2 (1.000 mg CeL^{-1}). Apesar da transferência de Ce nessa cadeia trófica, não foi constatada redução na sobrevivência e fecundidade dos afídeos.

Palavras Chave: nanotecnologia; Solanaceae; inseto; transferência trófica; espectroscopia por fluorescência de raios-X

In the last 20 years, there has been great development and use of nanotechnology in the electronics, automotive, energy, medicine, and agricultural sectors (Paschoalino et al. 2010; Vance et al. 2015). Several academic studies suggest that nanoCuO, nanoZnO, nanoCeO_2, and nano TiO_2 can be used in fertilization by seed treatment (Duran et al. 2017), or broadcast on foliage and soil (Raliya et al. 2018). Additionally, they also may be applied as pesticides (Khot et al. 2012).

Several efforts have been made to assess the fate of nanomaterials during and after the life cycle of the products. One of the difficulties in assessing the impacts of released nanoparticles regards its transformation along the lifecycle. During production, the materials are kept in a controlled environment, but once incorporated they can undergo reactions such as abrasion, combustion, etching, and photochemical change. Therefore, the pristine nanomaterials can yield different ones (Mitrano et al. 2015).

Although the models may diverge in points such as the concentration and chemical nature of released nanomaterials, they agree that the nanoparticles eventually might be found in the environment (Dwivedi et al. 2015; Ju-Nam & Lead 2016; Campolo et al. 2017). This means that they can be airborne, reach water instreams, or be adsorbed to soil colloids, and therefore interact with plants and animals.

Studies using pristine nanomaterials, such as the one presented in this paper, are important from a mechanistic point of view, and they represent the first step towards more complex investigations.

Once in the environment, nanomaterials can be absorbed, accumulated, or transformed by living organisms such as bacteria, plants, and animals (Maurer-Jones et al. 2013). Because new physical-chemical properties occur at nanoscale (Talapin & Shevchenko 2016; Xu et al. 2018), the way in which nanomaterials affect these living organisms might be considerably different than their bulk counterparts. There-

[1]Universidade Federal de Lavras, Department of Entomology, Lavras, 37200-000, Minas Gerais, Brazil; E-mail: rosangelac.marucci@ufla.br (R. C. M.); larahmf@hotmail.com (L. M. F.); gacarval@ufla.br (G. A. C.)

[2]Universidade de São Paulo, Centre for Nuclear Energy in Agriculture, Piracicaba, 13400-970, São Paulo, Brazil; E-mail: joyceribeiro123@gmail.com (J. R. S. R.); hudson@cena.usp.br (H. W. P. C.)

[3]Universidade Tecnológica Federal do Paraná, COBIO, Santa Helena, 85892-000, Goiás, Paraná ,Brazil; E-mail: dejanealves@utfpr.edu.br (D. S. A.)

*Corresponding authors; E-mail: rosangelac.marucci@ufla.br; hudson@cena.usp.br

fore, specific studies aimed at investigating the effects of nanomaterials on living organisms are necessary to ensure their sustainable usage.

Together with nano ZnO, CuO, and Ag, CeO_2 is one the most-investigated nanomaterials. Due to its low redox potential and scratch resistance, it is used largely in catalysis (Montini et al. 2016) and as an abrasive (Dan et al. 2014). The application of metal oxide nanoparticles in agriculture is still at the research level. The results show that depending on the dose and nanoparticle physical-chemical features, the effects can be beneficial. Studies report increased seed germination rate (Duran et al. 2017), seedling development (Duran et al. 2018), biomass production (Raliya & Tarafdar 2013), and grain yield (Kottegoda et al. 2017).

On the other hand, previous investigations have shown that CeO_2 can be toxic to plants (Priester et al. 2012). Because nano-CeO_2 can be absorbed by roots and transported to plant shoots (Gomez-Garay et al. 2014) and grains (Hernandez-Viezcas et al. 2013), they potentially can be transferred to animals through herbivory.

Although the interaction between nano-CeO_2 and plants has been investigated, there is little information on effects of nano-CeO_2 on insects. Hawthorne et al. (2014) found Ce transfer from zucchini, *Cucurbita pepo* L. (Cucurbitaceae), plants to house crickets, *Acheta domesticus* L. (Orthoptera: Gryllidae), and further transfer from these crickets to spiders (Lycosidae). Majumdar et al. (2016) recently showed that Ce accumulated in the leaves of *Phaseolus vulgaris* L. (Fabaceae) can be transferred to Mexican bean beetle, *Epilachna varivestis* Mulsant (Coleoptera: Coccinellidae). Both studies indicated that most of the Ce ingested by the insects was excreted (about 98% of Ce consumed by the beetle); however, nearly 5-fold biomagnification was observed when the Mexican bean beetles were preyed upon by spined soldier bugs, *Podisus maculiventris* (Say) (Heteroptera: Pentatomidae).

The questions remain: (i) can CeO_2 nanoparticles be transferred from plants to piercing-sucking insects? and (ii) is there any toxic or behavioral effect to insects that feed on plants exposed to nano-CeO_2?

We used green peach aphid, *Myzus persicae* (Sulz.) (Hemiptera: Aphididae), as a model system in this work because of ease of rearing and handling. Additionally, it is a polyphagous species that infests hundreds of species from 40 plant families (Blackman & Eastop 2007), is an effective vector of phytopathogens, and has worldwide distribution (Blackman & Eastop 2000; Malais & Ravensberg 2003). In addition, this sucking insect feeds on the sap of the plants, which makes it a possible target for exposure to contaminated plants, and an indicator of the transfer of nanoparticles.

Nicandra physaloides (L.) Pers. (Solanaceae) was selected as a model plant because it is widely distributed, fast growing, produces sufficient aerial biomass to feed primary consumers, and is fed upon by green peach aphid. The primary objective of this study was to investigate the possible transfer of nano-CeO_2 across 2 trophic levels in a terrestrial food chain, using *N. physaloides* plants as a producer, and green peach aphid, *M. persicae*, as a representative piercing-sucking herbivore.

Materials and Methods

NANOPARTICLE CHARACTERISTICS AND SUSPENSION PREPARATION

The nano-CeO_2 was purchased from MK Nano (Toronto, Ontario, Canada) in powder form. The supplier indicated that particles are 25 nm wide and 99.9% pure. The particles were dispersed in deionized water with a probe sonic dismembrator (Model 705, Fisher Scientific, Pittsburgh, Pennsylvania, USA) at 95 watts, 50 Joules amplitude for 2 cycles of 3 min each, and interval of 30 s each cycle, yielding a stock dispersion at 1,000 mg Ce L^{-1}. Transmission electron microscopy images for CeO_2 were acquired to determined particle size and shape. A CeO_2 aqueous dispersion was prepared in deionized water at 1,000 mg Ce L^{-1}. The images were recorded using a JEM-1011 transmission electron microscope (Carl Zeiss AG, Oberkochen, Germany) operating at 60 Kv with the scales of the electromicrographs printed directly.

DYNAMIC LIGHT SCATTERING

The particle size in the aqueous dispersion was determined by dynamic light scattering. The measurements were performed using a Zetasizer Nano (Malvern Instruments, Malvern, Worcestershire, United Kingdom). In addition to the stock dispersion, we also measured dispersions at 100, 10, and 1 mg Ce L^{-1}.

PLANTS

Nicandra physaloides seeds were obtained from Universidade Federal de Lavras, Lavras, Minas Gerais State, Brazil. They were sown in 3 L pots containing a mixture of field collected soil (3 parts red Latosol soil plus 1 part cattle manure). The plants were maintained in a greenhouse and watered daily. They were used in the bioassays after 35 d, when the plants were about 50 cm in height.

INSECTS

Green peach aphids, *M. persicae*, were obtained from a colony at the Entomology Department of Universidade Federal de Lavras, Lavras, Minas Gerais State, Brazil. The insects were reared on leaves of sweet pepper, *Capsicum annuum* L. (Solanaceae), placed under a layer of 1% agar-water in Petri dishes (15 cm diam), and kept at 22 ± 1 °C, 70 ± 10% RH, and 12:12 h (L:D) photoperiod. The sweet pepper leaves were changed 3 times per wk. To obtain insects of the same age, 5 adult females were transferred to each Petri dish, where they remained for 48 h. Females were removed, and first and second instars (48-h-old) of the same generation were used in the bioassays.

TROPHIC TRANSFER BIOASSAY

The foliage of *Nicandra physaloides* plants was sprayed with the treatments using hand sprayers. Nano-CeO_2 aqueous suspensions (1, 10, 100, and 1,000 mg Ce L^{-1}) were prepared by sonication as described above. We used distilled water in the dilutions of the suspensions, and in the negative control to simulate an exposure via irrigation water. The volume of spray applied per plant was approximately 5 mL, sufficient volume not to cause discharge (run-off). Five plants were used per treatment.

Four h after the plants were sprayed, first and second instar aphids were transferred to the plants. The insects were confined in acrylic cages (27 mm diam × 10 mm height) fixed on young upper leaves. Ten nymphs were transferred to each plant, 5 on each of 2 leaves.

The bioassay was maintained in a growth chamber (Fitotron - Eletrolab®, Piracicaba, São Paulo, Brazil) with 14:10 h (L:D) photoperiod, 24 ± 2 °C day and night temperature, and 60 ± 10% RH. The pots were watered daily, and aphid survival was evaluated daily. The total number of nymphs per female was counted from d 3 to 10 after the beginning of the bioassays. The number of nymphs was determined by dividing the number of nymphs in each cage by the number of females that survived in the respective cage.

All nymphs were removed from the cages daily and transferred to Petri dishes (15 cm diam) containing the leaves of *N. physaloides* taken from the same plant that fed the adult females. The leaves were placed

under a layer of 1% agar-water. After 3 to 4 d, the nymphs of this generation reached adulthood.

The aphids from each replicate that remained until the end of the test were stored in microcentrifuge tubes and frozen. The leaves of *N. physaloides* plants were pressed and dried until they were scanned by microprobe X-ray fluorescence spectroscopy.

CERIUM DETECTION

The spatial distribution of Ce was determined using micro-probe X-ray fluorescence spectroscopy (μ-XRF, EDAX equipment, Orbis PC, Mahwah, New Jersey, USA). Leaf samples and aphids were put on a sample holder consisting of a cuvette covered with 7.5 μm polyamide film. X-rays were generated by a rhodium anode operating at 30 kV and 700 μA. All maps were recorded using a 32 × 25 matrix of pixels. For the aphids, the beam size was focused on the sample yielding a spot size of 30 μm and 250 μm thick. An aluminum primary filter was used to improve the signal to noise ratio. The dwell time for grouped aphids was 10 s and for a single individual 6 s.

For the leaf maps, the aluminum filter was not used; they were recorded with dwell times of 2 s and 3 s for large (1 mm beam) and small (30 μm beam) areas, respectively. The calculation of instrumental threshold for maps, which is equivalent to the limit of detection, is presented elsewhere (Rodrigues et al. 2018). In this study, only the count rates values above 10 σ of the mean background were considered signals.

STATISTICAL ANALYSIS

The survival data of the insects were submitted to survival analysis with the Weibull model, with the Survival package (Therneau 2018) in software R® (R Development Core Team 2018). In addition, the Kolmogorov-Smirnov adhesion test was performed, in order to verify the fit of the data to the model. The data referring to the number of nymphs were analyzed by non-parametric Kruskal-Wallis analysis by the Pgirmess package (Giraudoux 2018) in the software R® (R Development Core Team 2018).

Results

BIOLOGICAL EFFECTS IN APHIDS

Nano-CeO_2 did not reduce the survival of *M. persicae* in our experiments. The mean survival ranged between 93.9 and 98.0% (χ^2 = 1.18; df = 4; *P* = 0.88) (Table 1) for all nano-CeO_2 concentrations, and in the negative control. The adherence test of Kolmogorov-Smirnov indicated that data fit to the model (D = 0.083; *P* = 0.3752). This finding shows that the application of different concentrations of nano-CeO_2 in the *N. physaloides* plants did not cause mortality to the aphid.

The treatments did not affect the fecundity of aphids; no difference in the total number of nymphs produced by each female was observed (χ^2 = 5.6292; df = 4; *P* = 0.2286). The mean number of nymphs ranged from 26 to 43 between the third and tenth d of evaluation (Fig. 1).

CHARACTERIZATION OF THE SUSPENSIONS AND CHEMICAL MAPPING OF APHIDS AND PLANTS

Dynamic light scattering was used to evaluate the hydrodynamic radius of the suspended nanoparticles (Table 2). Regardless of the putative individual particle size of 25 nm, in aqueous dispersion the nanoparticles were aggregated. The diam of aggregates varied from 110 ± 34 nm up to 266 ± 56 nm. The aggregation occurs due to Van der Walls attractive forces, and this behavior was verified previously by other researchers (Pusey 2002). Due to the low solubility of CeO_2 nanoparticles, the aggregate size is an important parameter because it eventually defines the porous tissue barriers through which aggregates can pass, and therefore which organs of the aphid can be reached (Brunner et al. 2006).

The transmission electron microscopy images shown in Fig. 2 indicate that the CeO_2 nanoparticles are spherical in shape. The histogram shows the frequency distribution of CeO_2 nanoparticle size. The average of size is 23 ± 7 nm, which confirms the manufacturer's information (MK Nano, Toronto, Ontario, Canada; 25 nm).

Figure 3 overlays a picture of a *N. physaloides* leaf and the corresponding chemical image, uncovering the spatial distribution of Ce in samples that received foliar application of nano-CeO_2 (1,000 mg Ce L^{-1}). Figure 3(a) shows a large area map (about 414 mm^2) which corresponds to about 40% of the leaf area. Figure 3(b) depicts a map of a smaller area (1.68 mm^2), but because the number of pixels were the same, it yielded higher lateral resolution when zooming in to a hot-spot of Ce on the leaf. The count scale shown in the figures is directly proportional to the Ce concentration; nonetheless, they cannot be directly compared because the data shown in Figure 3(a) was recorded with an X-ray spot of 1 mm, whereas that in Figure 3(b) was taken at 30 μm. Figure 3(a) shows that despite the Ce dispersion obtained by application by a sprayer, the spatial distribution of Ce at the leaf was not homogeneous. On the contrary, it seems that during drying the Ce tended to accumulate in certain regions. A similar effect called "coffee stain" is observed frequently while trying to obtain homogeneous thin films of nanoparticles by drop casting (Majumder et al. 2012), because evaporation velocity is higher at the borders of the droplets (line of contact with the surface) than at the center. Because no surfactants were employed to disperse the particles, the surface tension may have aggregated the droplets, leading to the hot-spots shown in Figure 3(a).

Table 1. Lethal mean time (TL_{50})*, survival (%), and values of α** and β***for Weibull distribution of *Myzus persicae* that were fed with *Nicandra physaloides* plants sprayed with different concentrations of nano-CeO_2.

Concentration (mg L^{-1})	TL_{50}*	% survival^{ns}	α**	β***
0	> 240 h	93.95	2230.48	1.24
1	> 240 h	95.97	3118.25	1.24
10	> 240 h	95.96	3112.98	1.24
100	> 240 h	98.00	5521.81	1.24
1,000	> 240 h	95.02	2620.09	1.24

* = Lethal mean time (TL_{50}).
** = parameter of scale.
*** = parameter of shape.
ns = not significant at the significance level of 5% for the Weibull distribution, where $S(t) = \exp(-(time/\delta)^{\alpha})$, δ = shape parameter; α =scale parameter.

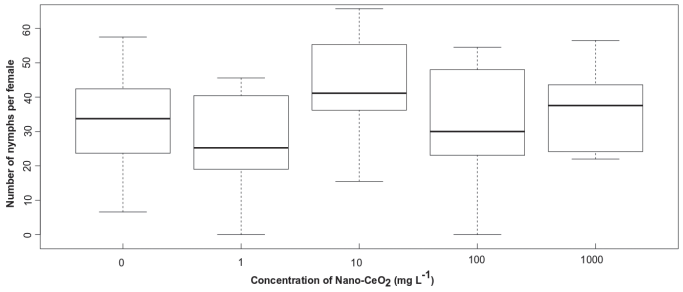

Fig. 1. Total number of *Myzus persicae* nymphs produced by females exposed to *Nicandra physaloides* leaves submitted to treatments of foliar spraying of nano-CeO_2 at different concentrations.

The limits of detection for Ce used in Figure 3(a) was 804 mg Ce kg^{-1} of fresh tissue. If any traces of Ce below this concentration were spread on the leaf, it would not be possible to detect them. Figure 3(b) shows that near a large Ce hot-spot, we can observe smaller and less concentrated droplets of Ce. The red spots in this chemical image also show the border effect caused by non-homogeneous drying. In this case, the limit of detection was 158 mg Ce kg^{-1} of fresh tissue. This improvement of the limit of detection resulted from the higher acquisition time and lower spectral (or instrumental) background provided by the polycapillary optics.

Ce was detected only in aphids that were fed with *N. physaloides* leaves sprayed with nano-CeO_2 (1,000 mg Ce L^{-1}). Figure 4(a) shows 4 aphids and corresponding chemical images showing the spatial distribution of Ce. It is possible to observe the Ce X-ray fluorescence signal coming from the regions corresponding to the oral cavity and digestive system of aphids. The detection threshold in terms of counts per s was 42 counts per s for the map shown in Figure 4(a). There was only 1 point in which Ce was above this value, and the corresponding spectrum shown in Figure 4(b) confirms the presence of Ce.

Figure 4(c, d) present similar results, and confirm that Ce was transferred to the aphids. In this case, the detection threshold was 53 counts per s. The difference in threshold between the maps shown in Figure 4(a) and 4(c) resulted from the different dwell time employed in each map.

The low number of counts indicates that there was little Ce in the aphids. In the other concentrations tested (1, 10, and 100 mg Ce L^{-1}), it was not possible to detect Ce in either plants or insects.

Discussion

We confirmed the hypothesis that nano-CeO_2 sprayed on the leaves of *N. physaloides* can be transferred to *M. persicae*. The presence of the Ce X-ray fluorescence spectroscopy signal in the abdomen of *M. persicae* and its absence in the legs suggested that nano-CeO_2 may have been absorbed by the insect rather than being retained on its body surface. This is the first report of the trophic transfer of nano-CeO_2 to a piercing-sucking insect, namely *M. persicae*.

Table 2. Dynamic light scattering determined hydrodynamic diam of suspended CeO_2 nanoparticles. Although the particles size is 25 nm, when dispersed in water they formed aggregates.

Concentration of CeO_2 (mg L^{-1})	Aggregate diam (nm ± SE)
1	220 ± 67
10	110 ± 40
100	110 ± 34
1,000	266 ± 56

Even though chemical images show the presence of Ce on the leaves, we cannot state whether the nano-CeO_2 was present on the surface or within the leaves. Several studies investigated the foliar uptake of nanoparticles, and neither the mechanisms behind the phenomenon nor size exclusion limits are clear yet (Larue et al. 2012; Raliya et al. 2016; Xiong et al. 2017).

Because *M. persicae* is a piercing-sucking insect that feeds on the phloem sap, at first glance one might assume that the source of nano-CeO_2 was within the leaf. However, we cannot reject the possibility that the insect absorbed the nano-CeO_2 that was on the leaf surface during successive feeding probes (Etxeberria et al. 2016). Prior to establishing a fixed feeding site, the aphid may make successive probing insertions of its stylets into the phloem vessels, a process marked by walking and selection of other probing sites (Tjallingii & Prado 2001). Thus, before the selection of the plant itself occurs, the aphids carry out many short probes at various points in the plant. During this process, it is possible that the stylets may have contacted the surface of the plant several times, which may have allowed the ingestion of the nano-CeO_2 deposited on the surface of the leaves of *N. physaloides*.

Even though Ce was found only at the region of the alimentary trait, one cannot reject the possibility of nano-CeO_2 clusters below the instrumental limit of detection that may accumulate in other parts of the body of *M. persicae*. In this case, nano-CeO_2 either could be dissolved in the alimentary canal, or entire particles could cross the gut wall. Due to the gut pH, from 5.5 to 8.5 depending on the site (Cristofoletti et al. 2003), it is rather unlikely to dissolve at gut pH. For cerium oxide to dissolve, low pH and high temperatures normally are required (Virot et al. 2012; Um & Hirato 2013).

A second possible Ce pathway is based on previous studies involving the transport of particles through the gut wall to the hemocoel, which commonly occurs with viruses (Brault et al. 2007; Tamborindeguy et al. 2010). Although most of the aphid-transmitted plant viruses are 20 to 25 nm wide (Sicard et al. 2015; Boissinot et al. 2017), which is about one-tenth the diam of nano-CeO_2 clusters, this transport is performed by transcytosis (endocytosis/exocytosis) (Seddas et al. 2004), and involves specific receptors. In this respect, nano-CeO_2 could cause histological changes in the tissues of *M. persicae*, similar to what was reported in a study performed with the worm *Eisenia fetida* (Savigny) (Annelida: Lumbricidae) (Lahive et al. 2014), resulting in absorption and transport.

Another mechanism by which nanoparticles may affect insects involves their interaction with symbiont microorganisms (Goggin 2007), which play a key role in aphid fitness, because they provide nutrients that occur in low amounts in the plant phloem. These microorganisms are commonly found in the hemocoel, in specialized cells called bacteriocytes or mycetocytes, or even in the gut lumen (Michalik et al. 2014; Luna-Ramirez et al. 2017). Thus, one can consider the possibility that microorganisms can transform nano-CeO_2 (Barton et al. 2015), or that the nanomaterial is toxic to these microorganisms, resulting in changes in the behavior of insects (Machado-Assefh & Alvarez 2018).

Although no toxic effects of nano-CeO_2 were observed in *M. persicae*, it is possible that the trophic transfer of nanoparticles causes damage to organisms of higher trophic levels through biomagnification. This was not evaluated in the present study, but this topic will be addressed in further investigations. Another issue of concern is the potential effects of nano-CeO_2 on the offspring of *M. persicae*, especially if exposed repeatedly over generations.

Gold nanoparticles previously have accumulated in the leaves of tobacco, *Nicotiana tabacum* L. (Solanaceae) (Judy et al. 2011), and

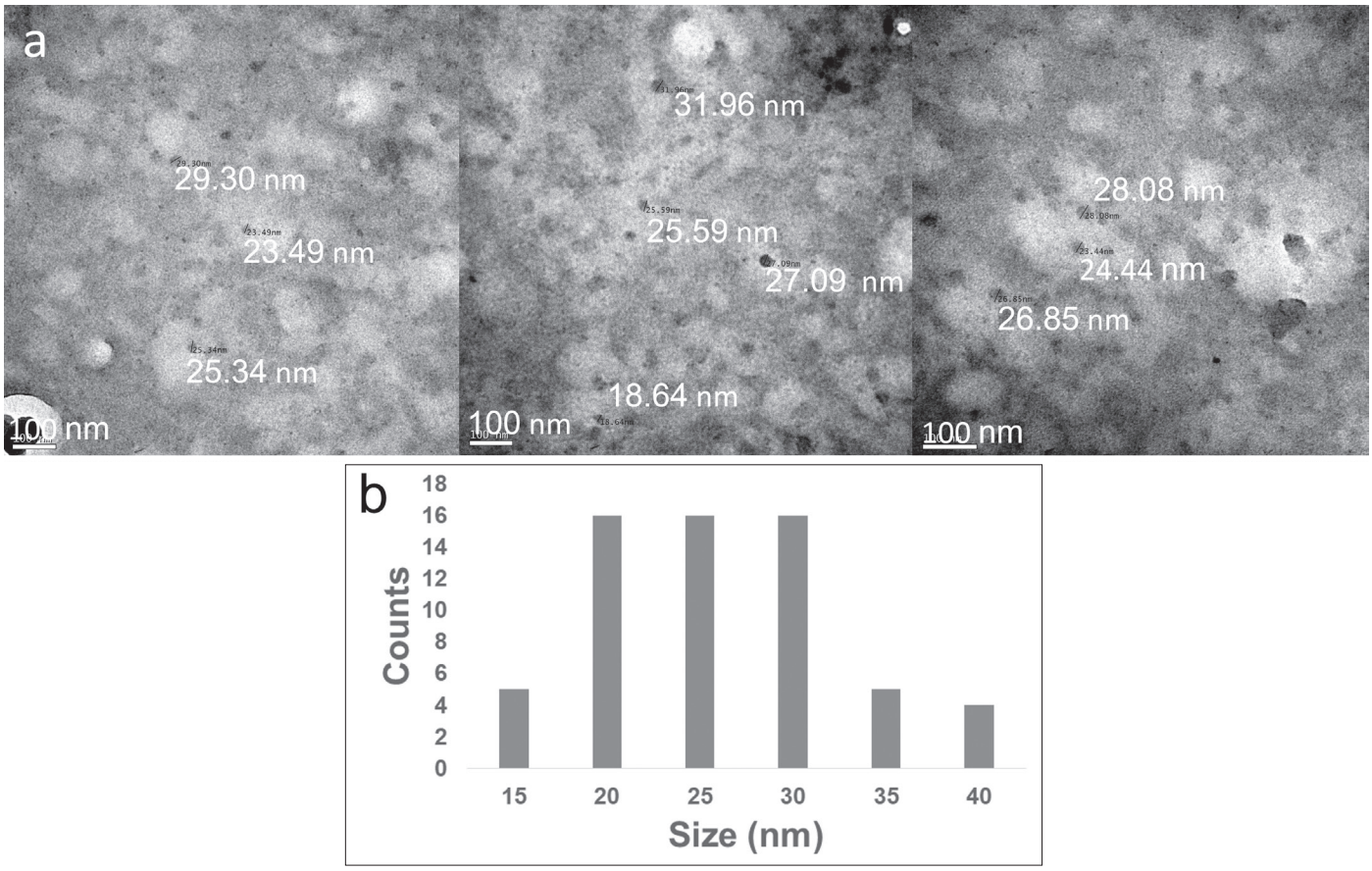

Fig. 2. (a) Transmission electron micrographs of the CeO_2 nanoparticles, and (b) histogram revealing the particle size distribution.

tomato, *Solanum lycopersicum* L. (Solanaceae) (Judy et al. 2012), and have been shown to accumulate in the hornworm *Manduca sexta* L. (Lepidoptera: Sphingidae). Similar to the findings reported in this study with *M. persicae*, the authors concluded that *M. sexta* was not affected by the ingestion of plant tissues contaminated with nano-Au.

These results demonstrate the importance of research on nanomaterials in biological systems, because the indirect effects frequently are manifested in subsequent generations, resulting in disrupted development or mortality. The translocation of nanoparticles in plants, and the transfer and accumulation in organisms of the trophic chain, warrant further investigation.

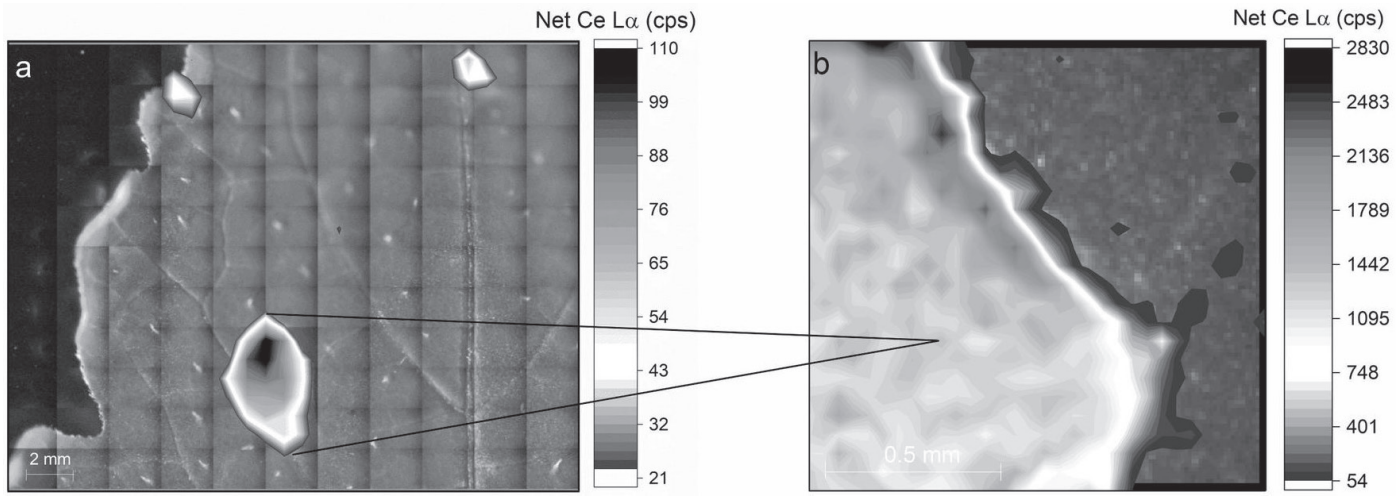

Fig. 3. X-ray fluorescence chemical images unraveling the Ce spatial distribution at *Nicandra physaloides* leaf, (a) low magnification (10×) map covering nearly a quarter of the leaf surface, and (b) high magnification (70×) map showing a hot-spot of Ce at the leaf.

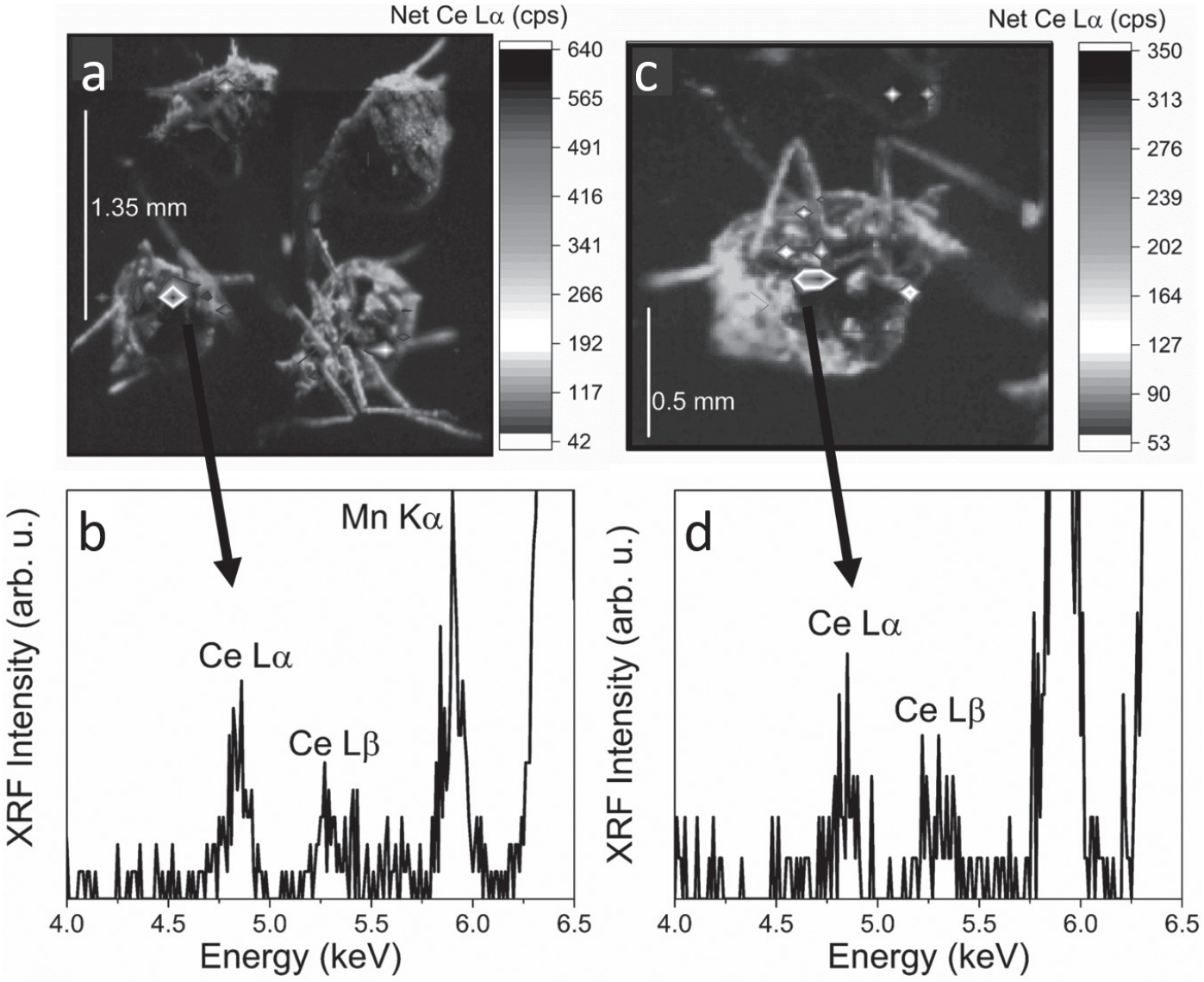

Fig. 4. Spatial distribution of Ce assimilated by *Myzus persicae* maintained in plants of *Nicandra physaloides* treated with nano-Ce (1,000 mg Ce L^{-1}): (a) presents a group of individuals; (b) shows the XRF spectrum with Ce Lα and Lβ lines corresponding to the hot-spot; (c) shows the map for 1 individual; (d) the corresponding XRF spectrum.

Acknowledgments

The authors are grateful to the São Paulo Research Foundation (FAPESP) for financial support through the programs "Young Investigators Awards" (2015/05942-0) and the "Multiuser Equipment Program" (2015/19121-8).

References Cited

Barton LE, Auffan M, Olivi L, Bottero JY, Wiesner MR. 2015. Heteroaggregation, transformation and fate of CeO_2 nanoparticles in wastewater treatment. Environmental Pollution 203: 122–129.

Blackman RL, Eastop VF. 2007. Taxonomic issues, pp. 192–199 *In* Emden HF, Van Harrington R [eds.], Aphids as Crop Pests. CAB International, Wallingford, United Kingdom.

Blackman RL, Eastop VF. 2000. Aphids on the World's Crops. An Identification and Information Guide. John Wiley & Sons, Chichester, United Kingdom.

Boissinot S, Pichon E, Sorin C, Piccini C, Scheidecker D, Ziegler-Graff V, Brault V. 2017. Systemic propagation of a fluorescent infectious clone of a polerovirus following inoculation by agrobacteria and aphids. Viruses 9: 166–184.

Brault V, Herrbach É, Reinbold C. 2007. Electron microscopy studies on luteovirid transmission by aphids. Micron 38: 302–312.

Brunner TJ, Wick P, Manser P, Spohn P, Grass RN, Limbach LK, Bruinink A, Stark WJ. 2006. In vitro cytotoxicity of oxide nanoparticles: comparison to asbestos, silica, and the effect of particle solubility. Environmental Science & Technology 40: 4374–4381.

Campolo O, Cherif A, Ricupero M, Siscaro G, Grissa-Lebdi K, Russo A, Cucci LM, Di Pietro P, Satriano C, Desneux N, Biondi A, Zappalà L, Palmeri V. 2017. Citrus peel essential oil nanoformulations to control the tomato borer, *Tuta absoluta*: chemical properties and biological activity. Scientific Reports 7: 1–10.

Cristofoletti PT, Ribeiro AF, Deraison C, Rahbé Y, Terra WR. 2003. Midgut adaptation and digestive enzyme distribution in a phloem feeding insect, the pea aphid *Acyrthosiphon pisum*. Journal of Insect Physiology 49: 11–24.

Dan G, Xie G, Luo J. 2014. Mechanical properties of nanoparticles: basics and applications. Journal of Physics D: Applied Physics 47: 13001. doi:10.1088/0022-3727/47/1/013001

Duran NM, Savassa SM, de Lima RG, Almeida E, Linhares FS, van Gestel CAM, Pereira de Carvalho HW. 2017. X-ray spectroscopy uncovering the effects of Cu based nanoparticle concentration and structure on *Phaseolus vulgaris* germination and seedling development. Journal of Agricultural and Food Chemistry 65: 7874–7884.

Duran NM, Medina-Llamas M, Cassanji JGB, De Lima RG, De Almeida E, Macedo WR, Mattia D, Pereira De Carvalho HW. 2018. Bean seedling growth en-

hancement using magnetite nanoparticles. Journal of Agricultural and Food Chemistry 66: 5746–5755.
Dwivedi AD, Dubey SP, Sillanpää M, Kwon YN, Lee C, Varma RS. 2015. Fate of engineered nanoparticles: implications in the environment. Coordination Chemistry Reviews 287: 64–78.
Etxeberria E, Gonzalez P, Borges AF, Brodersen C. 2016. The use of laser light to enhance the uptake of foliar-applied substances into citrus (*Citrus sinensis*) leaves. Applications in Plant Sciences 4: 1500106. doi: 10.3732/apps.1500106
Giraudoux P. 2018. Spatial analysis and data mining for field ecologists [R Package Pgirmess Version 1.6.9]. Comprehensive R Archive Network (CRAN). https://cran.r-project.org/web/packages/pgirmess/index.html (last accessed 15 May 2019).
Goggin FL. 2007. Plant-aphid interactions: molecular and ecological perspectives. Current Opinion in Plant Biology 10: 399–408.
Gomez-Garay A, Pintos B, Manzanera JA, Lobo C, Villalobos N, Martín L. 2014. Uptake of CeO_2 nanoparticles and its effect on growth of *Medicago arborea* in vitro plantlets. Biological Trace Element Research 161: 143–150.
Hawthorne J, Roche RT, Xing B, Newman LA, Ma X, Majumdar S, Gardea-Torresdey J, White JC. 2014. Particle-size dependent accumulation and trophic transfer of cerium oxide through a terrestrial food chain. Environmental Science & Technology 48: 13102–13109.
Hernandez-Viezcas JA, Castillo-Michel H, Andrews JC, Cotte M, Rico C, Peralta-Videa JR, Ge Y, Priester JH, Holden PA, Gardea-Torresdey JL. 2013. In situ synchrotron X-ray fluorescence mapping and speciation of CeO_2 and ZnO nanoparticles in soil cultivated soybean (*Glycine max*). ACS Nano 7: 1415–1423.
Judy JD, Unrine JM, Bertsch PM. 2011. Evidence for biomagnification of gold nanoparticles within a terrestrial food chain. Environmental Science & Technology 45: 776–781.
Judy JD, Unrine JM, Rao W, Bertsch PM. 2012. Bioaccumulation of gold nanomaterials by *Manduca sexta* through dietary uptake of surface contaminated plant tissue. Environmental Science & Technology 46: 12672–12678.
Ju-Nam Y, Lead J. 2016. Properties, sources, pathways, and fate of nanoparticles in the environment, pp. 93–117 *In* Engineered Nanoparticles and the Environment: Biophysicochemical Processes and Toxicity. John Wiley & Sons, Inc., Hoboken, New Jersey, USA.
Khot LR, Sankaran S, Maja JM, Ehsani R, Schuster EW. 2012. Applications of nanomaterials in agricultural production and crop protection: a review. Crop Protection 35: 64–70.
Kottegoda N, Sandaruwan C, Priyadarshana G, Siriwardhana A, Rathnayake UA, Berugoda Arachchige DM, Kumarasinghe AR, Dahanayake D, Karunaratne V, Amaratunga GAJ. 2017. Urea-hydroxyapatite nanohybrids for slow release of nitrogen. ACS Nano 11: 1214–1221.
Lahive E, Jurkschat E, Shaw BJ, Handy RD, Spurgeon DJ, Svendsen C. 2014. Toxicity of cerium oxide nanoparticles to the earthworm *Eisenia fetida*: subtle effects. Environmental Chemistry 11: 268–278.
Larue C, Veronesi G, Flank AM, Surble S, Herlin-Boime N, Carrière MM. 2012. Comparative uptake and impact of TiO_2 nanoparticles in wheat and rapeseed. Journal of Toxicology and Environmental Health, Part A 75: 722–734.
Luna-Ramirez K, Skaljac M, Grotmann J, Kirfel P, Vilcinskas A. 2017. Orally delivered scorpion antimicrobial peptides exhibit activity against pea aphid (*Acyrthosiphon pisum*) and its bacterial symbionts. Toxins 9: 1–16.
Machado-Assefh CR, Alvarez AE. 2018. Probing behavior of aposymbiotic green peach aphid (*Myzus persicae*) on susceptible *Solanum tuberosum* and resistant *Solanum stoloniferum* plants. Insect Science 25: 127–136.
Michalik A, Szklarzewicz T, Jankowska W, Wieczorek K. 2014. Endosymbiotic microorganisms of aphids (Hemiptera: Sternorrhyncha: Aphidoidea): ultrastructure, distribution and transovarial transmission. European Journal of Entomology 111: 91–104.
Majumdar S, Trujillo-Reyes J, Hernandez-Viezcas JA, White JC, Peralta-Videa JR, Gardea-Torresdey JL. 2016. Cerium biomagnification in a terrestrial food chain: influence of particle size and growth stage. Environmental Science & Technology 50: 6782–6792.
Majumder M, Rendall CS, Eukel JA, Wang JYL, Behabtu N, Pint CL, Liu TY, Orbaek AW, Mirri F, Nam J, Barron AR, Hauge RH, Schmidt HK, Pasquali M. 2012. Overcoming the 'coffee-stain' effect by compositional marangoni-flow-assisted drop-drying. The Journal of Physical Chemistry B 116: 6536–6542.
Malais MH, Ravensberg WJ. 2003. Knowing and Recognizing: The Biology of Glasshouse Pests and Their Natural Enemies. Reed Business Information, Doetinchem, The Netherlands.
Maurer-Jones MA, Gunsolus IL, Murphy CJ, Haynes CL. 2013. Toxicity of engineered nanoparticles in the environment. Analytical Chemistry 85: 3036–3049.
Mitrano DM, Motellier S, Clavaguera S, Nowack B. 2015. Review of nanomaterial aging and transformations through the life cycle of nano-enhanced products. Environment International 77: 132–147.
Montini T, Melchionna M, Monai M, Fornasiero P. 2016. Fundamentals and catalytic applications of CeO_2-based materials. Chemical Reviews 116: 5987–6041.
Paschoalino MP, Marcone GP, Jardim WF. 2010. Os nanomateriais e a questão ambiental. Química Nova 33: 421–430.
Priester JH, Ge Y, Mielke RE, Horst AM, Moritz SC, Espinosa K, Gelb J, Walker SL, Nisbet RM, An Y-J, Schimel JP, Palmer RG, Hernandez-Viezcas JA, Zhao L, Gardea-Torresdey JL, Holden PA. 2012. Soybean susceptibility to manufactured nanomaterials with evidence for food quality and soil fertility interruption. Proceedings of the National Academy of Sciences 109: E2451–E2456.
Pusey PN. 2002. Dynamic light scattering, pp. 203–205 *In* Lindner P, Zemb T [eds.], Neutrons, X-rays and Light: Scattering Methods Applied to Soft Condensed Matter. North-Holland, Amsterdam, The Netherlands.
R Development Core Team. 2018. R: The R Project for Statistical Computing. Vienna, Austria. https://www.r-project.org/ (last accessed 15 May 2019).
Raliya R, Saharan V, Dimkpa C, Biswas P. 2018. Nanofertilizer for precision and sustainable agriculture: current state and future perspectives. Journal of Agricultural and Food Chemistry 66: 6487–6503.
Raliya R, Franke C, Chavalmane S, Nair R, Reed N, Biswas P. 2016. Quantitative understanding of nanoparticle uptake in watermelon plants. Frontiers in Plant Science 7: 1288. https://doi.org/10.3389/fpls.2016.01288 (last accessed 15 May 2019).
Raliya R, Tarafdar JC. 2013. ZnO Nanoparticle biosynthesis and its effect on phosphorous-mobilizing enzyme secretion and gum contents in clusterbean (*Cyamopsis tetragonoloba* L.). Agricultural Research 2: 48–57.
Rodrigues ES, Gomes MHF, Duran NM, Cassanji JGB, da Cruz TNM, Sant'Anna Neto A, Savassa SM, de Almeida E, Carvalho HWP. 2018. Laboratory microprobe X-ray fluorescence in plant science: emerging applications and case studies. Frontiers in Plant Science 9: 1588. https://doi.org/10.3389/fpls.2018.01588 (last accessed 15 May 2019).
Seddas P, Boissinot S, Strub JM, Van Dorsselaer A, Van Regenmortel MHV, Pattus F. 2004. Rack-1, GAPDH3, and actin: proteins of *Myzus persicae* potentially involved in the transcytosis of beet western yellows virus particles in the aphid. Virology 325: 399–412.
Sicard A, Zeddam J, Yvon M, Michalakis Y. 2015. Circulative non-propagative aphid transmission of nanoviruses. Journal of Virology 89: 9719–9726.
Talapin DV, Shevchenko EV. 2016. Introduction: nanoparticle chemistry. Chemical Reviews 116: 10343–10345.
Tamborindeguy C, Monsion B, Brault V, Hunnicutt L, Ju HJ, Nakabachi A, Van Fleet E. 2010. A genomic analysis of transcytosis in the pea aphid, *Acyrthosiphon pisum*, a mechanism involved in virus transmission. Insect Molecular Biology 19: 259–272.
Therneau TM. 2018. Survival Analysis [R Package Survival Version 2.41-3]. Comprehensive R Archive Network (CRAN). https://cran.r-project.org/web/packages/survival/index.html (last accessed 15 May 2019).
Tjallingii WF, Prado E. 2001. Analysis of circulative transmission by electrical penetration graphs, pp. 69–85 *In* Harris K, Smith O, Duffus J [eds.], Virus-Insect-Plant Interactions. Academic Press, San Diego, California, USA.
Um N, Hirato T. 2013. Dissolution behavior of La_2O_3, Pr_2O_3, Nd_2O_3, CaO and Al_2O_3 in sulfuric acid solutions and study of cerium recovery from rare earth polishing powder waste via two-stage sulfuric acid leaching. Materials Transactions 54: 713–719.
Vance ME, Kuiken T, Vejerano EP, McGinnis SP, Hochella MF, Rejeski D, Hull MS. 2015. Nanotechnology in the real world: redeveloping the nanomaterial consumer products inventory. Beilstein Journal of Nanotechnology 6: 1769–1780.
Virot M, Chave T, Horlait D, Clavier N, Dacheux N, Ravaux J, Nikitenko SI. 2012. Catalytic dissolution of ceria under mild conditions. Journal of Materials Chemistry 22: 14734–14740.
Xiong TT, Dumat C, Dappe V, Vezin H, Schreck E, Shahid M, Pierart A, Sobanska S. 2017. Copper oxide nanoparticle foliar uptake, phytotoxicity, and consequences for sustainable urban agriculture. Environmental Science & Technology 51: 5242–5251.
Xu L, Liang HW, Yang Y, Yu SH. 2018. Stability and reactivity: positive and negative aspects for nanoparticle processing. Chemical Reviews 18: 3209–3250.